

# Bose Condensation by Gravitational Interactions

D.G. Levkov,<sup>1,2,\*</sup> A.G. Panin,<sup>1,2</sup> and I.I. Tkachev<sup>1,3</sup>

<sup>1</sup>*Institute for Nuclear Research of the Russian Academy of Sciences, Moscow 117312, Russia*

<sup>2</sup>*Moscow Institute of Physics and Technology, Dolgoprudny 141700, Russia*

<sup>3</sup>*Novosibirsk State University, Novosibirsk 630090, Russia*

We study Bose condensation and formation of Bose stars in the virialized dark matter halos/miniclusters by universal gravitational interactions. We prove that this phenomenon does occur and it is described by kinetic equation. We give expression for the condensation time. Our results suggest that Bose stars may form in the mainstream dark matter models such as invisible QCD axions and Fuzzy Dark Matter.

*1. Introduction.* Bose stars are lumps of Bose condensate bounded by self-gravity [1, 2]. They can be made of condensed dark matter (DM) bosons — say, invisible QCD axions [3] or Fuzzy DM [4]. That is why physics, phenomenology and observational signatures of these objects remain in the focus of cosmological research for decades [5], see recent papers [6, 7]. Unfortunately, formation of Bose stars is still poorly understood and many recent works have to assume their existence.

In this Letter we study Bose condensation in the virialized DM halos/miniclusters caused by universal gravitational interactions. We work at large occupation numbers which is correct if the DM bosons are light. Notably, we consider kinetic regime where the initial coherence length and period of the DM particles are close to the de Broglie values  $(mv)^{-1}$  and  $(mv^2)^{-1}$  and much smaller than the halo size  $R$  and condensation time  $\tau_{gr}$ ,

$$mvR \gg 1, \quad mv^2\tau_{gr} \gg 1. \quad (1)$$

We numerically solve microscopic equations for the gravitating “gas” of bosons in this case and find that the Bose stars indeed form. We derive expression for  $\tau_{gr}$  and study kinetics of the process.

Up to our knowledge, gravitational Bose condensation in kinetic regime has not been observed before. Old works considered only contact interactions between the DM bosons [8] which are non-universal and suppressed by quartic constants  $\lambda \sim 10^{-50}$  [9] and  $10^{-100}$  [10] in models of QCD axions and string axions/Fuzzy DM. Our results show that in these cases gravitational condensation is *faster*: although the Newton’s constant  $Gm^2$  is tiny, its effect is enhanced by collective interaction of large fluctuations in the boson gas at large distances, cf. [11].

On the other hand, all previous numerical studies of Bose star formation considered coherent initial configurations of the bosonic field — a Gaussian wavepacket [12] or the Bose star itself [13]. A spectacular simulation of structure formation by wavelike/Fuzzy DM [14] started from (almost) homogeneous Bose condensate. In all these cases the Bose stars may form almost immediately [12, 13] from the lowest-energy part of the initial condensate. We study entirely different situation (1) when the DM bosons are virialized in the initial state.

We do not consider scenario [11, 15] with axions forming cosmological condensate at the radiation-dominated stage because it was envisaged outside of the regime (1).

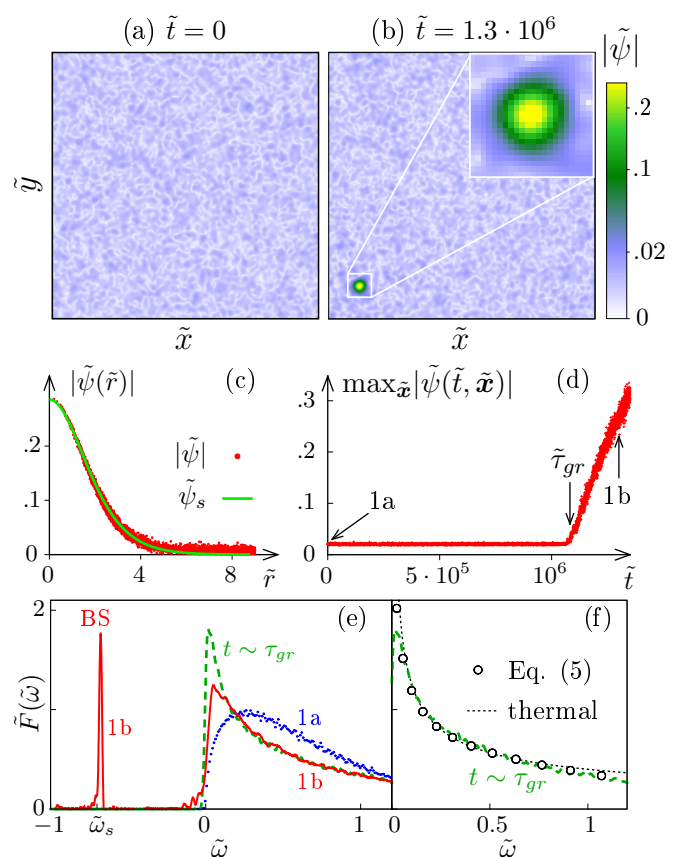


FIG. 1. Formation of a Bose star from a random field with initial distribution  $|\tilde{\psi}_{\vec{p}}|^2 \propto e^{-\vec{p}^2}$  and total mass  $\tilde{N} = 50$  in the box  $0 \leq \tilde{x}, \tilde{y}, \tilde{z} < 125$ . These values correspond to the center of axion minicluster in Sec. 8 with  $M_c \sim 10^{-13} M_\odot$  and  $\Phi \sim 2.7$ . (a), (b) Sections  $\tilde{z} = \text{const}$  of the solution  $|\tilde{\psi}(\tilde{t}, \tilde{\mathbf{x}})|$  at (a)  $\tilde{t} = 0$  and (b)  $\tilde{t} > \tilde{\tau}_{gr} \approx 1.07 \cdot 10^6$ . (c) Radial profile  $|\tilde{\psi}(\tilde{r})|$  of the object in Fig. 1b (points) compared to the Bose star  $\tilde{\psi}_s(\tilde{r})$  with  $\tilde{\omega}_s \approx -0.7$  (line). (d) Maximum of  $|\tilde{\psi}(\tilde{\mathbf{x}})|$  over the box as a function of time. (e) Spectra (3) at times of Figs. 1a, b and at the eve of Bose star nucleation,  $\tilde{t} = 1.05 \cdot 10^6 \sim \tilde{\tau}_{gr}$ . (f) The spectrum at  $t \sim \tau_{gr}$  (dashed line) versus solution of Eq. (5) (circles) and thermal law  $\tilde{F} \propto \tilde{\omega}^{-1/2}$  (dots).

2. *The birth of the Bose star.* Consider  $N$  nonrelativistic gravitationally interacting bosons in a periodic box of size  $L$ . At large occupation numbers this system is described by a random classical field  $\psi(t, \mathbf{x})$  [8] evolving in its own gravitational potential  $U(t, \mathbf{x})$ ,

$$\begin{aligned} i\partial_t\psi &= -\Delta\psi/2m + mU\psi, \\ \Delta U &= 4\pi Gm(|\psi|^2 - n), \end{aligned} \quad (2)$$

where the mean particle density  $n \equiv N/L^3$  is subtracted in the second line for consistency [14]. Notably, Eqs. (2) simplify in dimensionless variables: substitutions  $\mathbf{x} = \tilde{\mathbf{x}}/mv_0$ ,  $t = \tilde{t}/mv_0^2$ ,  $U = v_0^2\tilde{U}$  and  $\psi = v_0^2\tilde{\psi}\sqrt{m/G}$  exclude parameters  $m$  and  $G$  from the equations and reference velocity  $v_0$  — from the initial conditions. The rescaled particle number is  $\tilde{N} \equiv \int d^3\tilde{\mathbf{x}}|\tilde{\psi}|^2 = Gm^2N/v_0$ .

We fix initial conditions in the momentum space. A representative class of them describes Gaussian-distributed bosons,  $|\tilde{\psi}_{\tilde{\mathbf{p}}}|^2 = 8\pi^{3/2}\tilde{N}e^{-\tilde{\mathbf{p}}^2}$ , with random arg  $\tilde{\psi}_{\tilde{\mathbf{p}}}$ . Fourier-transforming  $\tilde{\psi}_{\tilde{\mathbf{p}}}$ , we obtain an isotropic and homogeneous initial configuration  $\tilde{\psi}(0, \tilde{\mathbf{x}})$  with minimal coherence length in Fig. 1a. Then we numerically evolve Eqs. (2) using an exceptionally stable 3D algorithm [16], see movie [19]. Apart from the erratic motion of  $\psi$ -peaks and deeps, nothing happens for a long time  $t < \tau_{gr}$ , where  $\tilde{\tau}_{gr} \sim 10^6$  for the solution in Fig. 1. Then suddenly a coherent, compact and spherically symmetric object appears at  $t > \tau_{gr}$ , see Fig. 1b. With time the object grows in mass and moves in a Brownian way.

To explain what happens, we recall that any interaction between the bosons should lead to thermal equilibrium, and in the case of large occupation numbers — to formation of a Bose condensate. Gravitational interaction is not an exception [11]. But then the condensate cannot appear in a homogeneous state [15]. Rather, it should fragment due to Jeans instability into a set of isolated Bose stars, cf. [8], which is therefore the actual end-state of the condensation process.

The field profiles of the Bose stars are found by solving Eqs. (2) with the spherical Ansatz  $\psi = \psi_s(r)e^{-i\omega_s t}$  at each  $\omega_s < 0$ , see e.g. [20]. The exemplary star is shown in Fig. 1c (line). It coincides with the profile of the object in Fig. 1b (points) thus proving that we indeed observe nucleation of a Bose star caused by gravitational interactions. We performed simulations for a large set of parameters, for  $\delta$ - and  $\theta$ -like initial distributions,  $|\psi_{\tilde{\mathbf{p}}}|^2 \propto \delta(|\tilde{\mathbf{p}}| - mv_0)$  and  $\theta(mv_0 - |\tilde{\mathbf{p}}|)$ , in addition to the Gaussian. Every time we observed formation of a Bose star with correct profile. Note that the Bose star radius is inversely proportional to its mass  $M_s$ , while  $\psi_s(0) \propto M_s^2$  [20]. Thus, these objects nucleate wide and rarefied, then shrink and become dense as they accumulate bosons. Unlike in other studies, no “seed” Bose condensate was present in our simulations at  $\tau < \tau_{gr}$ , otherwise it would grow above the background in a short time, see Fig. 1d.

3. *The spectrum.* To look deeper into the initial, seemingly featureless stage of gas evolution, we compute distribution  $F(t, \omega) = dN/d\omega$  of bosons over energies  $\omega$ . This quantity equals to Fourier image of the correlator

$$F = \int \frac{dt_1}{2\pi} d^3\mathbf{x} \psi^*(t, \mathbf{x})\psi(t + t_1, \mathbf{x}) e^{i\omega t_1 - t_1^2/\tau_1^2} \quad (3)$$

in kinetic regime  $(mv_0^2)^{-1} \ll \tau_1 \ll \tau_{gr}$  [21]. In dimensionless calculations we use  $\tilde{F} = mv_0^2 F/N$  normalized to unity:  $\int \tilde{F} d\tilde{\omega} = 1$ , where  $\tilde{\omega} = \omega/mv_0^2$ .

Figure 1e shows that the spectrum (3) completely changes during evolution at  $t < \tau_{gr}$ . It starts from a wide bell  $\tilde{F} \propto \tilde{\omega}^{1/2} e^{-2\tilde{\omega}}$  corresponding to Gaussian distribution in momenta in Fig. 1a. As the time goes on,  $F$  develops a peak at low  $\omega$  and becomes close to thermal at intermediate energies,  $F \propto \omega^{-1/2}$ , see the graph at  $t \sim \tau_{gr}$  in Figs. 1e and 1f. Once the Bose star nucleates, a  $\delta$ -peak appears in the distribution, see the spectrum 1b in Fig. 1e. This  $\delta$ -peak is formed by condensed particles of energy  $\omega_s < 0$  inside the star. It starts close to  $\omega \approx 0$  at  $t = \tau_{gr}$  and moves to the left as the Bose star grows.

Below we use the  $\delta$ -peak at  $\omega < 0$  as an indicator of Bose star nucleation: we define  $\tau_{gr}$  as the moment when the peak is twice higher than the fluctuations in  $F(t, \omega)$ .

4. *Condensation time.* In kinetic regime evolution of  $F(t, \omega)$  is described by kinetic equation — this fact can be proven [18] by solving Eqs. (2) perturbatively and using approximations (1), cf. [21]. Below we confirm the same fact numerically. One therefore expects that the time of Bose star formation  $\tau_{gr}$  is proportional with some coefficient  $b$  to the kinetic relaxation time:  $\tau_{gr} = 4b\sqrt{2}/(\sigma_{gr}vnf)$ , where  $\sigma_{gr} \approx 8\pi(mG)^2\Lambda/v^4$  is the transport Rutherford cross section of gravitational scattering,  $\Lambda = \log(mvL)$  is the Coulomb logarithm, and  $f = 6\pi^2n/(mv)^3 \gg 1$  is the phase space density that appears due to Bose stimulation [8]. The coefficient  $b = O(1)$  accounts for the details of the process. It is expected to depend weakly on the initial distribution.

Taking all factors together, we obtain expression

$$\tau_{gr} = \frac{b\sqrt{2}}{12\pi^3} \frac{mv^6}{G^2n^2\Lambda}, \quad b \sim 1 \quad (4)$$

that apart from the Coulomb logarithm involves only local parameters i.e. the boson number density  $n$  and velocity  $v$ . So, up to weak logarithmic dependence on the size  $L$  formation of a Bose star can be regarded as a local process, with periodic box representing a central part of some DM halo. We will confirm this intuition below.

We performed simulations of the gas with Gaussian initial distribution at different  $\tilde{L}$  and  $\tilde{n}$ . Our results for  $\tau_{gr}$  (circles in Fig. 2a) cover two orders of magnitude, but they are nevertheless well fitted by Eq. (4) with  $v = v_0$  and  $b \approx 0.9$  (upper line in Fig. 2a). To confirm that Eq. (4) is universal, we repeated the calculations for the initial  $\delta$ -distribution,  $|\psi_{\tilde{\mathbf{p}}}|^2 \propto \delta(|\tilde{\mathbf{p}}| - mv_0)$  (squares in

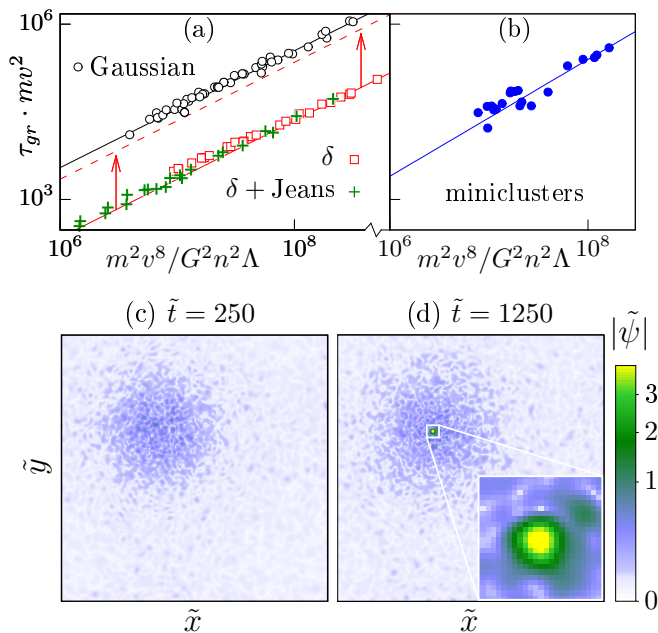


FIG. 2. (a) Time to Bose star formation in the cases of Gaussian (o) and  $\delta$ -peaked ( $\square$ ) initial distributions, as well as  $\delta$ -distributions developing Jeans instabilities during kinetic evolution ( $+$ ). The  $\delta$ -graphs are shifted downwards ( $\tau_{gr} \rightarrow \tau_{gr}/10$ ) for visualization purposes. Lines depict fits by Eq. (4). (b) The same for isolated miniclusters. (c), (d) Slices  $\tilde{z} = \text{const}$  of the solution  $|\tilde{\psi}(\tilde{t}, \tilde{\mathbf{x}})|$  describing formation of a Bose star in the center of a minicluster;  $\tilde{N} = 290$ ,  $\tilde{L} \approx 63$ .

Fig. 2a). The new values of  $\tau_{gr}$  are still described by Eq. (4), albeit with slightly different coefficient  $b \approx 0.6$ . We conclude that Eq. (4) is a practical justified expression for the time of Bose star formation.

5. *Kinetics.* Let us show that evolution of  $F(t, \omega)$  in Fig. 1e is indeed governed by the Landau kinetic equation [22] for homogeneous ensemble of gravitating waves,

$$\partial_t \tilde{F} = \tau_0^{-1} \partial_{\tilde{\omega}} \left[ A \partial_{\tilde{\omega}} \tilde{F} + (B \tilde{F} - A) \tilde{F} / 2\tilde{\omega} \right]. \quad (5)$$

Here the scattering integral in the right-hand side involves  $A(\tilde{\omega}) = \int_0^\infty d\tilde{\omega}_1 \min^{3/2}(\tilde{\omega}, \tilde{\omega}_1) \tilde{F}^2(\tilde{\omega}_1) / (3\tilde{\omega}_1 \tilde{\omega}^{1/2})$ ,  $B(\tilde{\omega}) = \int_0^{\tilde{\omega}} d\tilde{\omega}_1 \tilde{F}(\tilde{\omega}_1)$ , it is explicitly proportional to the inverse relaxation time  $\tau_0^{-1} = 8\pi^3 n^2 G^2 (\Lambda + a) / mv_0^6 \sim \tau_{gr}^{-1}$ . Notably, Eq. (5) is valid in the leading logarithmic approximation  $\Lambda \gg 1$  which is too rough for our numerical solutions with  $\Lambda \sim 5$ . To get a quantitative comparison, we added an unknown correction  $a = O(1)$  to  $\Lambda$ .

We numerically evolve Eq. (5) starting from the same initial distribution as in Fig. 1. In Fig. 1f the solution  $F(\tau_{gr}, \omega)$  (circles) is compared to the microscopic distribution (3) (dashed line) at  $t \approx \tau_{gr}$ , where  $a \approx 5$  is obtained from the fit. We observe agreement in the kinetic region  $\tilde{\omega} \gg 2\pi^2 / \tilde{L}^2$  which confirms that Eq. (5) correctly describes evolution at  $t < \tau_{gr}$ .

Note that unlike in the case of short-range interac-

tions [23] thermalization in Landau equation does not proceed via simple power-law turbulent cascades [22], and we do not observe them in Figs. 1e,f. Nevertheless, we think that Eq. (5) provides the basis for analytic description of gravitational Bose condensation.

6. *Miniclusters.* So far we assumed that homogeneous gas in the box correctly describes central parts of DM halos. Now, we study the isolated halos/miniclusters themselves and verify this assumption. Recall that in large volume nonrelativistic gas clumps at scales  $R \gtrsim 2\pi/k_J$  due to Jeans instability, where  $k_J^2 = 2\pi G n m^2 \langle \omega^{-1} \rangle$  and the average is computed with  $F(\omega)$ . Starting numerical evolution from the homogeneous gas with  $\delta$ -distributed momenta at  $L > 2\pi/k_J$ , we indeed observe formation of a virialized minicluster in Fig. 2c. With time it remains stationary until a Bose star appears in its center, see Fig. 2d and movie [19]. Thus, formation of Bose stars is not specific to finite boxes.

We checked that our kinetic expression for  $\tau_{gr}$  works for the virialized miniclusters. To this end we generated many different miniclusters, computed their central densities  $n$  and virial velocities  $\langle v^2 \rangle = -2\langle \omega \rangle / m$  using the  $\omega < 0$  part of the distribution  $F(\omega)$ , estimated their radii  $R$ . In Fig. 2b we plot the times of Bose star formation in the miniclusters versus these parameters and  $\Lambda = \log(mvR)$  (points). The numerical data are well approximated by Eq. (4) with  $b \approx 0.7$  (line) although the statistical fluctuations are now larger due to limited control over momentum distribution inside the miniclusters.

Estimating the virial velocity  $v^2 \sim 4\pi G m n R^2 / 3$  in the halo of radius  $R$ , one recasts Eq. (4) in the intuitively simple form  $\tau_{gr} \sim 0.047 (R/v) (Rmv)^3 / \Lambda$ , where the numerical factor is computed. Remarkably,  $\tau_{gr}$  equals to the free-fall time  $R/v$  multiplied by the cube of kinetic constant  $Rmv \gg 1$  in Eq. (1). In non-kinetic case  $Rmv \sim 1$  the Bose stars form immediately [12–14].

If  $L$  is a bit smaller than  $2\pi/k_J$  at  $t = 0$ , the virialized miniclusters form during the condensation process. Indeed, kinetic evolution shifts  $F(\omega)$  to smaller  $\omega$ , so  $k_J$  grows with time. Once  $k_J = 2\pi/L$  is reached, a minicluster of size  $R \sim L$  appears and subsequent condensation proceeds in its center. We find that in this case Eq. (4) with *original* values of  $v$  and  $n$  is still valid, see the crosses in Fig. 2a. Indeed, solving equation  $k_J = 2\pi/L$ , one finds that Jeans instability occurs when the typical velocity in the box is comparable to the virial velocity inside the minicluster. Thus, Eq. (4) approximately holds both in terms of the minicluster and of the original box.

7. *Bose star growth.* After nucleation the Bose stars start to acquire particles from the gas. Due to computational limitations we are able to observe only the first decade of their mass increase that proceeds according to the heuristic law  $M_s(t) \simeq cv_0(t/\tau_{gr} - 1)^{1/2} / Gm$  with  $c = 3 \pm 0.7$ . The ratio  $t/\tau_{gr}$  in this expression suggests that growth of the Bose stars is a kinetic process deserving a separate study.

8. *Discussion.* Let us argue that the Bose stars appear in the popular cosmological models. If the DM is made of invisible QCD axions [3] they have to form in the centers of axion miniclusters [24, 25], the smallest substructures of typical mass  $M_c \sim 10^{-13} M_\odot$  resulting from inhomogeneous QCD phase transition. The miniclusters are characterized [25] by the ratio  $\Phi + 1 \equiv n/\bar{n}|_{RD}$  of their central density  $n$  to the cosmological axion density  $\bar{n}$  at the radiation-dominated stage when they are still in the linear regime. Using parameters of late gravitationally bound miniclusters [25] in Eq. (4) and expressing the result in terms of  $\Phi$  and  $M_c$ , we find,

$$\tau_{gr} \sim \frac{10^9 \text{ yr}}{\Phi^3(1+\Phi)} \left( \frac{M_c}{10^{-13} M_\odot} \right)^2 \left( \frac{m}{26 \mu\text{eV}} \right)^3,$$

where the reference values of  $m$  and  $M_c$  are taken from [9] and [26]. Thus, typical miniclusters with  $\Phi \sim 1$  condense during the lifetime of the Universe, the densest ones with  $\Phi \sim 10^3$  [25] — in several hours. The Bose stars are important [6] as they hide a part of DM from observations. After becoming large they may explode into relativistic axions [7] or emit radiophotons via parametric resonance [2, 18] which at different redshifts may explain FRB [27] and anomalies of ARCADE 2 and EDGES [28].

Note that gravitational relaxation of QCD axions is significantly faster than relaxation due to self-coupling  $\lambda \equiv m^2/f^2$ , where  $f \sim 10^{11}$  GeV is the Peccei-Quinn scale. Indeed, in kinetic regime the ratio of the relaxation rates is proportional to that of the cross sections,  $\tau_{self}/\tau_{gr} \sim \sigma_{gr}/\sigma_{self} \sim (10fG^{1/2}/v)^4$ . In typical miniclusters  $v \sim 10^{-10} \ll 10fG^{1/2}$  and gravitational interactions win by  $\tau_{self}/\tau_{gr} \sim 10^{12}$ .

Another popular class of DM models is based on string axions / Fuzzy DM [4]. An interesting though recently constrained [29] scenario considers the smallest mass  $m \sim 10^{-22}$  eV of these particles [14] when their de Broglie wavelength inside the dwarf galaxies is comparable to the size of the galaxy cores,  $mvR \sim 1$ . As we argued, the Bose stars should appear in these cores in free-fall time. This explains their fast formation [14] in numerical simulations. At larger masses one substitutes typical parameters of dwarf satellites into Eq. (4),

$$\tau_{gr} \sim 10^6 \text{ yr} \left( \frac{m}{10^{-22} \text{ eV}} \right)^3 \left( \frac{v}{30 \text{ km/s}} \right)^6 \left( \frac{0.1 M_\odot/\text{pc}^3}{\rho} \right)^2.$$

The Bose stars nucleate there if  $m \lesssim 2 \cdot 10^{-21}$  eV, at the boundary of experimentally allowed mass window [29]. Then the missing satellites may hide as Bose stars. At even larger  $m$  the Bose stars may form in miniclusters and in cores of large galaxies, they may grow overcritical and explode [7]. Note that self-interaction of typical string axions [10] with  $f \sim 10^{-2} G^{-1/2}$  is less effective than gravity because  $v \ll 10fG^{1/2}$  in all structures.

We thank A. Pustynnikov, D. Gorbunov, M. Ivanov, E. Nugaev and V. Rubakov for discussions. This work was supported by the grant RSF 16-12-10494. Numerical calculations were performed on the Computational cluster of TD INR RAS.

---

\* levkov@ms2.inr.ac.ru

- [1] R. Ruffini, S. Bonazzola, Phys. Rev. **187**, 1767 (1969).
- [2] I. I. Tkachev, Sov. Astron. Lett. **12**, 305 (1986).
- [3] P. Sikivie, Lect. Notes Phys. **741**, 19 (2008).
- [4] A. Ringwald, Phys. Dark Univ. **1**, 116 (2012).
- [5] F. E. Schunck and E. W. Mielke, Class. Quant. Grav. **20**, R301 (2003)
- [6] J. Eby *et al*, JHEP **1612**, 066 (2016). P. S. B. Dev, M. Lindner and S. Ohmer, Phys. Lett. B **773**, 219 (2017). T. Helfer *et al*, JCAP **1703**, 055 (2017). J. Eby *et al*, JHEP **1704**, 099 (2017). E. Braaten, A. Mohapatra and H. Zhang, Phys. Rev. D **96**, 031901 (2017). P.-H. Chavanis, arXiv:1710.06268. L. Visinelli *et al*, Phys. Lett. B **777**, 64 (2018).
- [7] D. G. Levkov, A. G. Panin, and I. I. Tkachev, Phys. Rev. Lett. **118**, 011301 (2017).
- [8] I. I. Tkachev, Phys. Lett. B **261**, 289 (1991). S. Khlebnikov and I. Tkachev, Phys. Rev. D **61**, 083517 (2000).
- [9] V. B. Klaer and G. D. Moore, JCAP **1711**, 049 (2017).
- [10] A. Arvanitaki *et al*, Phys. Rev. D **81**, 123530 (2010).
- [11] P. Sikivie and Q. Yang, Phys. Rev. Lett. **103**, 111301 (2009). O. Erken *et al*, Phys. Rev. D **85**, 063520 (2012).
- [12] E. Seidel, W.-M. Suen, Phys. Rev. Lett. **72**, 2516 (1994).
- [13] H.-Y. Schive *et al*, Phys. Rev. Lett. **113**, 261302 (2014).
- [14] H.-Y. Schive *et al*, Nature Phys. **10**, 496 (2014).
- [15] A. H. Guth *et al*, Phys. Rev. D **92**, 103513 (2015).
- [16] We use 6th-order FFT integrator [17] with graphics processing units (GPU) acceleration. At each time step we solve the Poisson equation via FFT. The error of our method is  $O(\Delta t^6)$  in time and exponentially small in lattice spacing  $\Delta x$ . The method is stable due to exact conservation of particle number  $N$ . We use  $128^3$  or  $256^3$  lattices. Numerical details will be reported elsewhere [18].
- [17] H. Yoshida, Phys. Lett. A **150**, 262 (1990).
- [18] D. G. Levkov, A. G. Panin, and I. I. Tkachev, *to appear*.
- [19] [https://www.youtube.com/playlist?list=PLMxQF3HFStX0\\_CFowbYStkjRv-xZEG-Vn](https://www.youtube.com/playlist?list=PLMxQF3HFStX0_CFowbYStkjRv-xZEG-Vn)
- [20] P.-H. Chavanis, Phys. Rev. D **84**, 043531 (2011).
- [21] V. Zakharov, V. L'vov, and G. Falkovich, *Kolmogorov Spectra of Turbulence I. Wave Turbulence*, Springer Berlin Heidelberg, 1992.
- [22] V. E. Zakharov, V. I. Karas', Phys. Usp. **56**, 49 (2013).
- [23] D. V. Semikoz and I. I. Tkachev, Phys. Rev. Lett. **74**, 3093 (1995); Phys. Rev. D **55**, 489 (1997).
- [24] C. J. Hogan, M. J. Rees, Phys. Lett. B **205**, 228 (1988).
- [25] E. W. Kolb and I. I. Tkachev, Phys. Rev. Lett. **71**, 3051 (1993); Phys. Rev. D **49**, 5040 (1994); Astrophys. J. **460**, L25 (1996).
- [26] J. Enander, A. Pargner, and T. Schwetz, JCAP **1712**, 038 (2017).
- [27] I. I. Tkachev, JETP Lett. **101**, 1 (2015).
- [28] J. Kehayias, T. W. Kephart and T. J. Weiler, JCAP **1510**, 053 (2015). S. Fraser *et al*, arXiv:1803.03245.
- [29] V. Iršič *et al*, Phys. Rev. Lett. **119**, 031302 (2017). E. Armengaud *et al*, MNRAS **471**, 4606 (2017).